International Journal on Magnetic Particle Imaging
Vol 6, No 2, Suppl 1, Article ID 2009049, 3 Pages

Infinite Science Publishing

Proceedings Article

Dynamic concentration reconstruction for magnetic particle imaging using splines

C. Schmidt[1,*] · C. Brandt[1]

[1]Department of Mathematics, Universität Hamburg, Hamburg, Germany
[*]Corresponding author, email: christiane.schmidt@uni-hamburg.de

Abstract

4D Magnetic Particle Imaging (MPI) reconstructions with high temporal resolution are of high relevance for diagnostic purposes. In multi-patch measurements the data for single patches is not continuous. During the scan of one patch no data is acquired for the remaining patches. This impedes regularization by similarity of subsequent frames. We propose a method that models the dynamic tracer concentration with cubic B-splines which allows for reconstructions with high temporal resolution from only few frames. The time-dependent formulation of the concentration leads to a new formula for modeling the system matrix.

I Introduction

The purpose of magnetic particle imaging is the visualization of the tracer concentration in specific organs or vessels. Thus, images with high gradients or discontinuities at organ boundaries are expected. Describing the tracer concentration by a function c it is discontinuous in space. Furthermore, in a medical setting the tracer cannot appear instantaneously. It accumulates, is dissipated or flows through a volume covered by one voxel. Thus, the function c is continuously differentiable in time.

For MPI scans with multiple patches there are gaps in time for single patches (see Fig. 1). In between each scanning period of a patch there is at least a time span of $T\cdot(P-1)$ in which the other patches are scanned, where T is the scanning time for one patch and P is the number of patches. This makes the similarity of subsequent frames less attractive as a regularization method. Furthermore, patches of the same frame are scanned at different time points which can cause artifacts. An example is shown in Fig. 2A.

In this paper we model the dynamic tracer concentration as a cubic B-spline curve in time for each voxel to gain continuously differentiable reconstruction from a low number of scanned frames, to approximate the missing data for multiple patches and to reduce patch artifacts.

II Methods

The MPI forward problem in time can be written as

$$u(t) = \frac{d}{dt}\int_\Omega \bar{m}(r,t)c(r,t)dr^3. \tag{1}$$

This holds true under the assumption that the signal generated by the excitation field is filtered out completely and leaving out the permeability constant and coil sensitivity as it is also assumed to be constant [2]. In contrast to most literature [2], [3], [4], [5], since we are looking at dynamic tracer concentrations, in this paper the concentration c is considered to be time-dependent and its time derivative to be nonzero so that the forward problem can be described by

$$u(t) = \int_\Omega \frac{d\bar{m}}{dt}(r,t)c(r,t) + \bar{m}(r,t)\frac{dc}{dt}(r,t)dr^3. \tag{2}$$

10.18416/ijmpi.2020.2009049

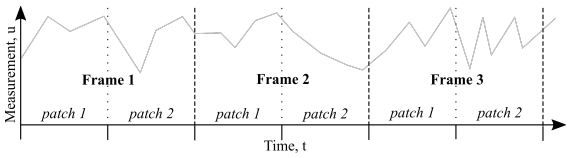

Figure 1: Scheme for scanning multiple patches. The measured voltage $u(t)$ is a concatenation of the measurements of all patches for each frame.

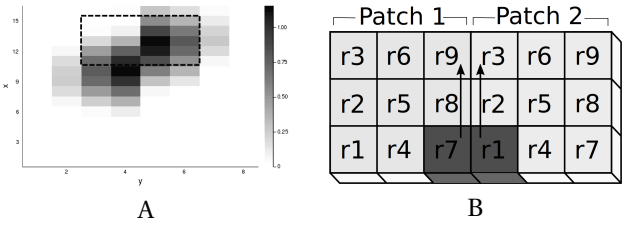

Figure 2: (A) Artifacts in multi-patch reconstruction for a phantom with linear motion in x. The two patches are scanned at different time points although they belong to the same frame. The outlines of the phantom at this time point are indicated by the dashed box. (B) Structure of the computational phantom with two patches and linear motion.

In [1] the authors deal with the dynamic inverse problem of gated cardiac SPECT (Single-photon emission computed tomography) reconstruction. In cardiac gating the periodic motion of the heart is divided into intervals, the so-called gates. They are interested in the decay of the radioactive tracer over time for each gate respectively. To achieve this they model the tracer concentration by cubic B-splines in time for each voxel. Based on this we model the particle concentration as

$$c_p(r,t) = \sum_{m \in M_p} b_m(r) B_m(t), \tag{3}$$

where p is the patch index, b_m are the control points and B_m are cubic B-splines. As we limit the reconstructed concentrations to those representable as spline curves this provides an implicit regularization. If the knots are chosen accordingly, this approach ensures differentiability in time, even for the periods without data for single patches. Discontinuity in space is still possible as there is a specific set of control points for each voxel.

We need to minimize the problem

$$\sum_{p=1} P \sum_{i=1}^{n_T} \| \sum_{j=1}^{R} \frac{d\bar{m}}{dt}(r_j,t_i) c_p(r_j,t_i) + \bar{m}(r_j,t_i) \frac{dc_p}{dt}(r_j,t_i) - u_p(t_i) \|_2^2 \tag{4}$$

with c_p defined as in (3) with respect to the set of all control points b_m. It can be minimized by a gradient descent or more advanced methods.

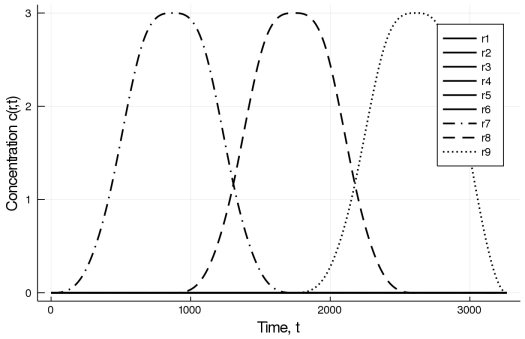

Figure 3: Patch 1 of a phantom with dynamic concentration. The curves show the development of the concentration in voxel r_i, $i \in 1,\ldots,9$ in time.

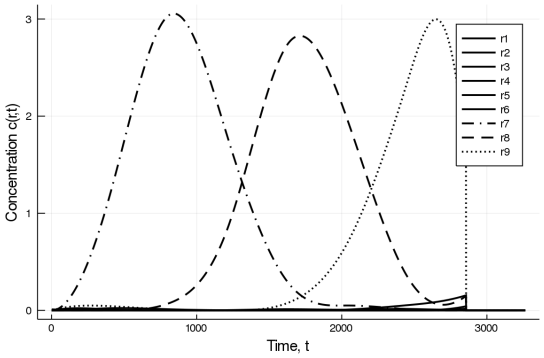

Figure 4: Reconstruction of patch 1 with the proposed method. Each curve shows the development of one voxel r in time.

III Results

The method was validated in a phantom study. The computational phantom has two patches which are aligned in y direction. Each patch consists of 3x3x1 voxels. The concentration moves nearly linear in positive x direction. The motion happens in parallel on both sides of the patch border (Fig.2 B). The concentration is modeled by spline curves. The development in time for each voxel of patch 1 can be seen in Fig. 3.

A scan with four frames was simulated. The system matrix was computed and the Lissajous trajectory was evaluated at 408 time points. The knots for the base splines are uniformly distributed in the sense that there are $M_0 = 5$ uniformly distributed knots in each scanning interval of the patch.

Additionally, there are quadruple knots at the beginning and end of the total scan time to allow discontinuities at these time points.

Problem (4) was solved with a gradient descent and an Armijo-type line search algorithm. The results can be seen in Fig. 4. The reconstruction is quite slow but results in reconstructions with a high temporal resolution. The

10.18416/ijmpi.2020.2009049

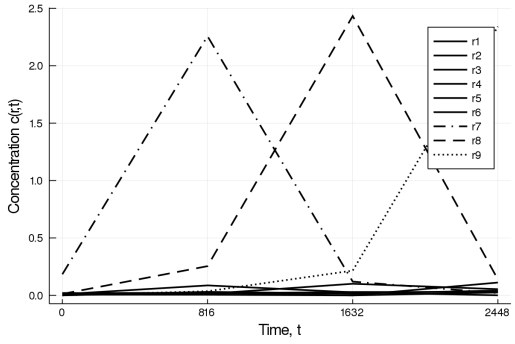

Figure 5: Reconstruction of patch 1 with the Kaczmarz method. The curves show the development of the concentration in voxel r_i, $i \in 1,\ldots,9$ in time.

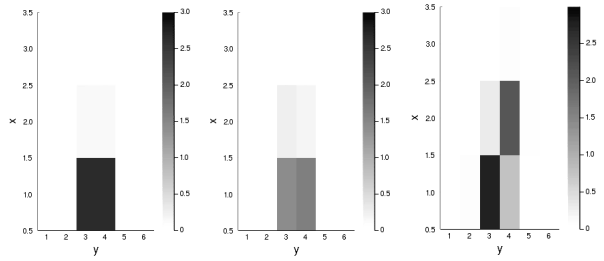

Figure 6: Phantom (left), spline based reconstruction (center) and frame-by-frame Kaczmarz reconstruction (right) shown at approximately the same time point.

development of the curves matches the ground truth quite well. Since the set of splines is slightly different the reconstruction cannot be exactly equal to the phantom.

For comparison the four frames were also reconstructed separately with the Kaczmarz algorithm. The results can be seen in Fig. 5. This reconstruction is more than twice as fast but has significantly lower temporal resolution. The reconstruction suffers from patch artifacts similar to the ones shown in Fig. 2A. Fig. 6 shows the phantom, the novel reconstruction method and the Kaczmarz approach at approximately the same time point.

IV Discussion

The introduced method is able to reconstruct dynamic tracer concentrations which are continuously differentiable in time and discontinuous in space with a high temporal resolution using measurements with a low number of scanned frames. It reduces artifacts caused by the subsequent scanning of patches by approximating the missing data.

For further improvement additional regularization terms and faster minimization algorithms can be added to speed up the reconstruction and to increase the quality of the reconstructions further. E.g. spatial sparsity can be enforced by a total variation term or mass conservation at patch borders. Depending on the regularization terms the problem can be solved by primal-dual algorithms.

References

[1] E. Gravier, et al., Tomographic reconstruction of dynamic cardiac image sequences, IEEE Trans. Image Processing, vol. 16, pp. 932–942, 2007.

[2] T. Knopp, T. Buzug, Magnetic Particle Imaging: An Introduction to Imaging Principles and Scanner Instrumentation, Springer Berlin Heidelberg, 2012.

[3] T. Kluth, Mathematical models for magnetic particle imaging, Inverse Problems 34.8:083001, 2018.

[4] T. Knopp, et al., Model-based reconstruction for magnetic particle imaging, IEEE Transactions on Medical Imaging, 29(1), 12-18, 2009

[5] W. Erb, et al., Mathematical analysis of the 1D model and reconstruction schemes for magnetic particle imaging, Inverse Problems, 34.5:055012, 2018.

